Dynamics and Thermodynamics of Water in PAMAM Dendrimers at Subnanosecond Time Scales

Shiang-Tai Lin, Prabal K. Maiti,† and William A. Goddard, III*

Materials and Process Simulation Center, California Institute of Technology, Pasadena, California 91125

Received: June 28, 2004; In Final Form: March 10, 2005

Atomistic molecular dynamics simulations are used to study generation 5 polyamidoamine (PAMAM) dendrimers immersed in a bath of water. We interpret the results in terms of three classes of water: buried water well inside of the dendrimer surface, surface water associated with the dendrimer−water interface, and bulk water well outside of the dendrimer. We studied the dynamic and thermodynamic properties of the water at three pH values: high pH with none of the primary or tertiary amines protonated, intermediate pH with only the primary amines protonated, and low pH with all amines protonated. For all pH values we find that both buried and surface water exhibit two relaxation times: a fast relaxation (∼1 ps) corresponding to the libration motion of the water and a slow (∼20 ps) diffusional component related to the escaping of water from one domain to another. In contrast for bulk water the fast relaxation is ∼0.4 ps while the slow relaxation is ∼14 ps. These results are similar to those found in biological systems, where the fast relaxation is found to be ∼1 ps while the slow relaxation ranges from 20 to 1000 ps. We used the 2PT MD method to extract the vibrational (power) spectrum and found substantial differences for the three classes of water. The translational diffusion coefficient for buried water is 11−33% (depending on pH) of the bulk value while the surface water is about 80%. The change in rotational diffusion is quite similar: 21−45% of the bulk value for buried water and 80% for surface water. This shows that translational and rotational dynamics of water are affected by the PAMAM−water interactions as well as due to the confinement in the interior of the dendrimer. We find that the reduction of translational or rotational diffusion is accompanied by a blue shift of the corresponding libration motions (∼10 cm^{-1} for translation, ∼35 cm^{-1} for rotation), indicating higher local force constants for these motions. These effects are most pronounced for the lowest pH, probably because of the increased rigidity caused by the internal charges. From the vibrational density of states we also calculate the enthalpies and entropies of the various waters. We find that water molecules are enthalpically favored near the PAMAM dendrimer: energy for surface water is ∼0.1 kcal/mol lower to that in the bulk, and ∼0.5−0.9 kcal/mol lower for buried water. In contrast, we find that both the buried and surface water are entropically unfavored: buried water is 0.9−2.2 kcal/mol lower than the bulk while the surface water is 0.1−0.2 kcal/mol lower. The net result is a thermodynamically unfavored state of the water surrounding the PAMAM dendrimer: 0.4−1.3 kcal/mol higher for buried water and 0.1−0.2 kcal/mol for surface water. This excess free energy of the surface and buried waters is released when the PAMAM dendrimer binds to DNA or metal ions, providing an extra driving force.

1. Introduction

Dendrimers constitute a class of highly branched polymers with distinct and unique structure and mechanical properties, making them interesting for theoretical research in addition to innovative applications. New dendrimers are continuing to be synthesized and studied, but the polyamidoamine (PAMAM) dendrimers, whose molecular structure is highly controllable and can be produced in a large quantity, continue to be particularly useful for many applications. Thus the low immunogenicity of PAMAM makes it a good candidate for biomedical applications such as gene and drug delivery.[1−3] Furthermore, the PAMAM dendrimers form stable complexes with metal ions[4−7] giving them potential applications for environmental cleanup and heavy metal recovery.

Despite extensive study, there remain questions on the atomistic 3-dimensional structure of PAMAM dendrimers, on which functional groups are protonated at different pH values, and on the mechanism for interacting with metal ions and such molecules as DNA. To address these issues systematically, we performed a series of molecular dynamic simulations,[8−10] focusing here on the dynamic and thermodynamic behavior of water in the PAMAM solution.

The dynamic properties of water in biological systems were found to exhibit two relaxation times:[11,12] a fast component (picosecond or subpicosecond) related to the librational motions of water and a slower component related to escaping of water molecules from the biomolecular surface to the bulk (the time scale of this relaxation depends on the specific molecules and the relaxation time ranges from a few picoseconds to hundreds of picoseconds). Such phenomena have been widely investigated by experiments[13−18] and by molecular simulations[19−26] for water in biological systems such as proteins and DNA.

* To whom correspondence should be addressed. E-mail: wag@wag.caltech.edu.

† Present address: Department of Physics, Indian Institute of Science, Bangalore 560012, India.

10.1021/jp0471958 CCC: $30.25
Published on Web 04/12/2005

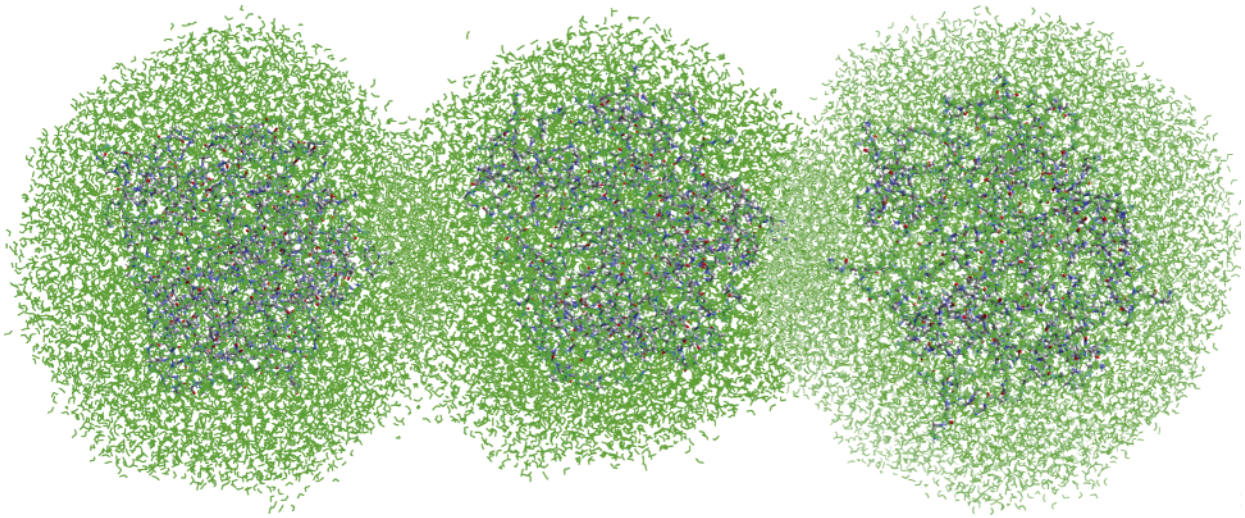

Figure 1. Snapshots of the equilibrated structure of G5 PAMAM dendrimers at different solution pH values. From left to right: high pH (no protonation), intermediate pH (128 primary amines protonated), low pH (128 primary and 126 tertiary amines protonated).

The difference in behavior of water near biomolecules compared to bulk waters has a great impact on the biological processes. For example, Bhattacharyya[18] showed that the slow relaxation of water leads to slow proton transfer for polar reactions taking place in biological assemblies. This results in a much higher reaction barrier with concomitant retardation in reactions. The slow water dynamics near the biomolecular surface also have significant implications for the protein−ligand binding and protein crystallization. It has been argued[13] that the picosecond time scale is ideal for protein−protein association. This would also be important for molecular recognition in water.

This paper reports a detailed analysis on the change of water dynamical properties near generation 5 (G5) PAMAM dendrimer in solutions with various pH values. We simulate three solution pH conditions: high pH (∼10) with none of the primary or tertiary amines protonated (neutral PAMAM); intermediate pH (∼7) with all 128 primary amines protonated, but none of the 126 tertiary amines protonated; and low pH (∼4) with all 254 amines protonated.

In addition we also report how the presence of PAMAM dendrimer affects the free energy of water under all these conditions. This study of free energies associated with buried water should aid in the understanding of the transport and binding of DNA and metals to PAMAM.

2. Computational Details

The initial atomistic structure of the PAMAM dendrimer at generation 5 was constructed by using the Continuous Configurational Boltzmann Biased (CCBB) Monte Carlo (MC) method.[9,27] This initial structure was then subjected to a series of protocols to accelerate equilibration of the structure. First, the conjugate gradient minimization was used to relax bad contacts in the CCBB generated structures. This minimized structure was then heated at a rate of 100 deg K/4 ps from 300 to 2000 K, followed by quenching to 1000 K at the same rate. This annealing cycle is repeated 4 times between 1000 and 2000 K, finally cooling to 300 K. This is followed by a long, 400 ps simulation in vacuum at 300 K. This room-temperature structure is immersed in a preequilibrated box of F3C water,[28] which gives satisfactory properties of bulk water at various temperatures. The water-box was extended 10 Å in each direction to ensure a complete solvation of the PAMAM molecule. To enhance the speed of simulation, we performed simulations for nonperiodic systems, i.e., the PAMAM is immersed in a large droplet of water. Therefore, our study may be subjected to additional surface effects when compared to biological systems in bulk.

The PAMAM water composite is then equilibrated for 200 ps at 300 K. The solution pH condition is specified by the level protonation of amines on the PAMAM dendrimer. At high pH (∼10) no protonation occurs. At neutral pH (∼7) all the 128 primary amines are protonated. At low pH (∼5), all the 128 primary amines and 126 tertiary amines are protonated.[29] For protonated PAMAM dendrimers, the protons are added before immersing them into water. Short minimization was performed to relax the added proton and its neighboring atoms. Appropriate amounts of chlorine counterions (Cl^-) are added near the protons to ensure charge neutrality. Snapshots of the water-solvated PAMAM structures are presented in Figure 1.

We used the generic Dreiding force fields[30] to describe the covalent (bond stretching, angle bending, torsion, and inversion) and van der Waals (Lennard-Jones 12-6) interactions for all atoms except for water, where the F3C force field parameters were used.

The atomic charges needed for describing the coulomb interactions are calculated from the charge equilibration (QEq) method.[31] First we evaluate the QEq charges for the EDA core, as a neutral molecule using generation 0, i.e., with all four terminal H atoms replaced by 4 monomers of PAMAM dendrimer. Then, we evaluate the QEq charges for the full monomer of PAMAM, with all three H atoms replaced by three monomers of PAMAM, again requiring charge neutrality. Finally we evaluate the QEq charges for the terminal PAMAM monomers, with the two terminal H atoms kept as H and the other H replaced a monomer of PAMAM dendrimer. These charges for the terminal PAMAM monomer were then scaled to be neutral and used for the terminal generation. This procedure ensures that each generation is neutral. In the case of neutral pH when all 128 primary amines are protonated, we found that the change of atomic charges is quite localized and can be specified by recalculating only the charges on the terminal monomer (including the 2nd monomer as described above), with a net charge of +1. However, for low pH where both primary and tertiary amines are protonated, we found that the effects cannot be contained within the monomer units. Thus for this case we determined the QEq charges for all atoms as a single molecule with the total charge constrained to +128.

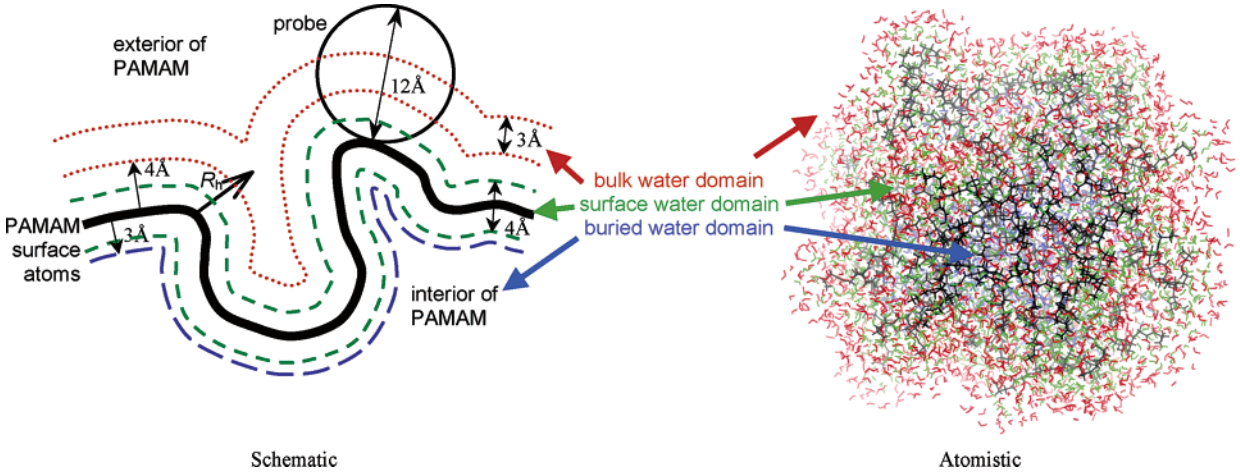

Figure 2. An illustration of water domains defined in this work

TABLE 1: Water Content and Solvent Excluded Surface (SES) Area of PAMAM Dendrimers at Different Solution pH Values

	domain				PAMAM SES
solution pH	overall N	buried	surface	bulk	area (Å^2)
high	9406	371 ± 17	1002 ± 16	1448 ± 24	10642 ± 185
intermediate	8948	543 ± 19	1345 ± 23	1789 ± 27	13216 ± 198
low	12977	738 ± 22	1726 ± 46	2507 ± 45	18526 ± 723

The long-range nonbonded Coulomb and van der Waals interactions are calculated by using the Cell Multipole Method (CMM).[32] The Verlet algorithm is used for velocity integration with the integration step set to 1 fs. The Nose-Hoover thermostat with a relaxation time constant of 0.01 ps is used for temperature control. All MD simulations and energy minimization were carried out with the MPSim molecular dynamics program.[33]

3. Results and Discussion

3.1. Definition of Water Regimes. To facilitate the analysis of the properties of water molecules, we define three spatial domains for the water in the PAMAM system: *buried*, *surface*, and *bulk*. First we construct the solvent excluded surface (SES) of the PAMAM dendrimer using a large probe radius of 6 Å (~4 times the radius of a water molecule). This is meant to distinguish between internal cavities with small necks (up to 12 Å in diameter) from broad concave regions that are not really internal. Then we define as *surface atoms* any that have a nonzero SES area. Then we define the *surface domain* as the space within a spherical radius of 2 Å from any surface atom. The *buried domain* is defined as the internal regime of PAMAM, 3 Å away from the surface atoms. The *bulk domain* is identified as an external shell of 3 Å thickness and 4 Å away from the PAMAM surface atoms. The water molecules that fall within each of the domains are identified as the *surface*, *buried*, *or bulk water* molecules, respectively. [In the computer program, surface water molecules are first identified by searching all the water molecules within 2 Å from PAMAM surface atoms. For each of the remaining water molecules, the distance between water and its closest PAMAM surface atom R_h is calculated. If R_h is greater than 3 Å and the water is inside PAMAM (judging from the outward normal on the PAMAM surface atom), the water molecule is labeled as buried. If R_h is less than 7 Å but greater than 4 Å, and the water is outside PAMAM, it is labeled as bulk. For clarity we illustrate this classification of waters in Figure 2.]

3.2. Residence Time of Water Molecules Inside and at the Surface of PAMAM Dendrimers. Defining $P_i^d(t)$ as the probability (either 0 or 1) of finding water molecule i in domain d (d = buried, surface, or bulk) at time t, we can study the rate of water molecules entering or exiting a domain through the following two time correlation functions

$$C_{cs}^d(t) = \sum_{i=1}^{N} \langle \prod_{t_k=0}^{t} P_i^d(t_k) \rangle \quad (1)$$

which provides the probability of a water molecule continuously staying (denoted by subscript cs) in domain d for a duration of time t, and

$$C_{re}^d(t) = \sum_{i=1}^{N} \langle P_i^d(t)\, P_i^d(0) \rangle \quad (2)$$

which allows for the re-entrance (denoted by subscript re) of the same water into a domain. The summation of i in eqs 1 and 2 runs over all the N water molecules (Table 1) within the system, and the notation $\langle\ \rangle$ indicates ensemble average and is determined by using the standard multiple origin sampling method from the trajectory. We have calculated and recorded $P_i^d(t)$ for each water molecule every 50 fs (i.e., $t_{k+1} - t_k = 50$ fs) from a 100 ps MD simulation run for PAMAM dendrimers at three different protonation levels. The $C^d(t)$ is calculated up to a maximum correlation time of 50 ps, i.e., 50% of the total trajectory.

Note that the values $NC^d(0)$ ($NC_{cs}^d(0) = NC_{re}^d(0)$) listed in Table 1 give the average water content within domain d for PAMAM systems at different protonation levels. It is noticeable that the water content in the buried and surface domains and PAMAM SES area increase with the PAMAM protonation level. This is consistent with previous findings that the radius of gyration of PAMAM increases (swollen) at low pH.[8,29]

The time evolution of normalized $C^d(t)$ for water in the neutral, unprotonated PAMAM solutions is depicted in Figure 3, parts a and b, and those of surface water and buried water around PAMAM at different protonation levels are compared in Figure 3, parts c−f. The water relaxation is determined by

TABLE 2: Water Relaxation Time Calculated Based on Eqs 1 and 3

		domain		
constants	solution pH	buried	surface	bulk
τ_f (ps)	high	1.161 ± 0.017	0.982 ± 0.011	0.318 ± 0.003
	intermediate	0.963 ± 0.014	1.009 ± 0.013	0.422 ± 0.006
	low	0.852 ± 0.013	0.854 ± 0.014	0.362 ± 0.004
τ_s (ps)	high	23.128 ± 0.243	4.268 ± 0.033	1.872 ± 0.003
	intermediate	13.948 ± 0.106	4.711 ± 0.030	2.394 ± 0.006
	low	9.284 ± 0.093	5.249 ± 0.029	2.275 ± 0.005
A_f	high	0.382 ± 0.001	0.413 ± 0.005	0.752 ± 0.001
	intermediate	0.432 ± 0.001	0.488 ± 0.004	0.689 ± 0.002
	low	0.350 ± 0.002	0.541 ± 0.003	0.699 ± 0.002
A_s	high	0.312 ± 0.002	0.532 ± 0.004	0.233 ± 0.001
	intermediate	0.398 ± 0.003	0.450 ± 0.004	0.285 ± 0.002
	low	0.512 ± 0.004	0.385 ± 0.003	0.276 ± 0.002
y_o	high	0.222 ± 0.001	0.003 ± 0.000	0.000 ± 0.000
	intermediate	0.069 ± 0.001	0.003 ± 0.000	0.001 ± 0.000
	low	0.022 ± 0.000	0.005 ± 0.000	0.001 ± 0.000
R^2	high	0.998	0.999	1.000
	intermediate	0.998	0.999	1.000
	low	0.996	0.999	1.000

TABLE 3: Water Relaxation Time Calculated Based on Eqs 2 and 3

		domain		
constants	solution pH	buried	surface	bulk
τ_f (ps)	high	0.186 ± 0.006	1.671 ± 0.035	1.482 ± 0.022
	intermediate	0.229 ± 0.007	1.868 ± 0.041	1.679 ± 0.029
	low	0.416 ± 0.013	1.810 ± 0.040	1.754 ± 0.030
τ_s (ps)	high	28.243 ± 0.383	18.277 ± 0.147	13.869 ± 0.175
	intermediate	24.078 ± 0.249	19.650 ± 0.168	13.887 ± 0.185
	low	18.650 ± 0.162	17.969 ± 0.149	14.481 ± 0.192
A_f	high	0.112 ± 0.001	0.471 ± 0.001	0.293 ± 0.002
	intermediate	0.172 ± 0.001	0.447 ± 0.001	0.298 ± 0.002
	low	0.253 ± 0.001	0.439 ± 0.001	0.298 ± 0.002
A_s	high	0.098 ± 0.002	0.212 ± 0.002	0.372 ± 0.003
	intermediate	0.132 ± 0.002	0.182 ± 0.002	0.323 ± 0.003
	low	0.161 ± 0.003	0.187 ± 0.002	0.316 ± 0.003
y_o	high	0.770 ± 0.001	0.219 ± 0.001	0.225 ± 0.001
	intermediate	0.661 ± 0.001	0.275 ± 0.001	0.265 ± 0.001
	low	0.510 ± 0.001	0.272 ± 0.001	0.268 ± 0.001
R^2	high	0.993	0.999	0.997
	intermediate	0.995	0.999	0.997
	low	0.996	0.999	0.997

fitting the normalized $C^d(t)$ to two exponential functions

$$\frac{C^d(t)}{C^d(0)} = A_f \exp\left(-\frac{t}{\tau_f}\right) + A_s \exp\left(-\frac{t}{\tau_s}\right) + y_0 \qquad (3)$$

It is found that the time correlation functions of water in the three regimes in the PAMAM systems at three protonation levels can be well described by using eq 3 as the correlation coefficients R^2 listed in Tables 2 and 3 are better than 0.99 in all cases.

In general, the water relaxation in the PAMAM system has a fast component (τ_f) at a time scale below 2 ps, and a slow component (τ_s) at 2 ps or longer. The fast component corresponds to the domain boundary water crossing or vibrating at the domain border. Such a fast vibrating mode is sometimes viewed as the water vibrating in a temporary cage formed by its neighboring molecules. Since allowing the re-entrance of water into the same domain (eq 2) misses some of the fast oscillations at the domain boundary, the residence time evaluated by using eq 1 provides the proper estimate of the fast mode relaxation. The fast mode relaxation time (τ_f) increases from about 0.4 ps for the bulk water to about 1 ps for the surface and buried water molecules (Table 2), indicating a drastic slowing down of water vibrations inside or at the surface of PAMAM. In the case of high solution pH, τ_f decreases by ~0.2 ps from surface (0.98 ps) to buried (1.16 ps). In the case of intermediate and low solution pH, the difference in τ_f between the surface and buried water is less than 0.05 ps. This is an indication of a very different environment inside a neutral (unprotonated) PAMAM dendrimer. In fact, this is consistent with our previous observation that the cavities inside neutral PAMAM dendrimers are more isolated and the protonation on amine groups opens up the buried cavities (Figure 1). The opening of the internal structure of the dendrimer makes the distinction between surface and buried domains less significant.

The slow relaxation component (τ_s) indicates the lifetime of water in the domain. In this case eq 2, which allows for water re-entrance and reduces the effect of the artificial choice of a rigid boundary, provides a better measurement of such relaxation. The slow mode relaxation time (τ_s) increases from about 14 ps for the bulk water to about 19 ps for surface water and 25 ps for buried water (Table 3). This, again, indicates a drastic slowing down of water relaxation inside or at the surface of PAMAM. It is noted that due to the open structure of PAMAM at low pH the residence time τ_s is only slightly increased (0.68 ps) from the surface water to buried water, whereas there is a much more significant change of residence time for the intermediate and high pH cases (4.43 and 9.97 ps, respectively).

Although the relaxation time τ_s from eq 1 is not very meaningful as this quantity is known to depend on the size and

shape (volume and surface area) of the domain,[21] the comparison of corresponding results from eq 2 provides insights to the re-entering behavior of water molecules into each domain. For example, the τ_s of surface water increases from about 5 ps using eq 1 to about 19 ps using eq 2, indicating a significant re-entrance of the same water into the same domain. In contrast, there is only a slight increase of τ_s (from 23 to 28 ps) for buried water under high solution pH. Such a difference is also caused by the more confined voids in the unprotonated PAMAM dendrimer, making the re-entrance of water more difficult.

We also note some small differences in τ_s and τ_f for bulk water under different solution pH values. Some chlorine ions (Cl^-) used to maintain charge neutrality in our simulation for intermediate and low pH cases apparently migrate into the bulk domain, making the water molecules behave slightly differently in different cases.

3.3. Change of Water Translation and Rotation Dynamics under Different Solution pH. The change of dynamical properties (translation and rotation) of water in different environments around PAMAM can be more clearly seen from the shift of the vibrational modes. The vibrational spectrum of water molecules can be determined from the Fourier transform of the velocity autocorrelation function[34,35]

$$S(\upsilon) = \frac{2}{kT}\lim_{\tau\to\infty}\int_{-\tau}^{\tau} C(t)\mathrm{e}^{-i2\pi\upsilon t}\,\mathrm{d}t \qquad (4)$$

where $C(t)$ can either be the mass weighted velocity autocorrelation function determined from the center of mass velocities $\upsilon^{CM}(t)$ of water molecules

$$C_T(t) = \sum_{i=1}^{n}\langle m_i \upsilon_i^{CM}(t)\cdot\upsilon_i^{CM}(0)\rangle \qquad (5)$$

or the moment of inertia weighted angular velocity autocorrelation function

$$C_R(t) = \sum_{j=1}^{3} c_{R_j}(t) = \sum_{j=1}^{3}\sum_{i=1}^{n}\langle I_{ij}\omega_{ij}^{CM}(t)\omega_{ij}^{CM}(0)\rangle \qquad (6)$$

where I_{ij} and ω_{ij}(t) are the jth principal moment of inertia and angular velocity of water molecule i.

It should be noted that the integration of the vibrational spectrum $S(\upsilon)$ over the entire frequency ($\upsilon = 0$ to ∞) gives the total degrees of freedom $3n$ of the system where n is the number of water molecules used in the summation in eqs 5 and 6. Furthermore, the zero frequency intensity $S(0)$ corresponds to the translational and rotational diffusion of water molecules[35]

$$D_T = \frac{kTS_T(0)}{12mn} \qquad (7)$$

and

$$D_R = \frac{kT\sum_{j=1}^{3} s_{R_j}(0)}{4n\sum_{j=1}^{3} I_j} \qquad (8)$$

The vibrational spectrum of water in the three domains is calculated for PAMAM dendrimers under different solution pH conditions. Previous analysis shows that, allowing the re-entrance of water molecules into the same domain, the residence time is about 20 ps (14 ps for bulk water, 19 ps for surface water, and 19−28 ps for buried water). We therefore identify the water in each domain at time zero (after the system is equilibrated) and save the velocity information of the same water molecules every 4 fs for 20 ps. Using 10 ps as the maximum correlation time, we obtain the vibration spectrum with a resolution of 1.1 cm^{-1}. The same analysis is repeated 5 times, which amounts to a total of 100 ps MD run for each case, to estimate the uncertainty in our analysis.

The translational and vibrational spectra of water are presented in Figure 4. It should be noted that all the spectra are normalized to one molecule, therefore the area underneath each curve is 3 (i.e., 3 translational or rotational degrees of freedom). The general feature of the translational mode distribution is the finite intensity at $\upsilon = 0$ cm^{-1}, and then increasing to a maximum at 30−65 cm^{-1}, followed by a monotonic decrease extending to more than 400 cm^{-1}. It can be seen that the surface and buried water are distinct from the bulk water by having a smaller value of $S_T(0)$ and a blue shift in the peak of librational motions. For the unprotonated (high pH) and primary amine protonated (intermediate pH) PAMAM dendrimers (Figure 4a,c), there is a significant decrease of $S_T(0)$ of water at the dendrimer surface, indicating a slower translational diffusion. The diffusion is even slower for the buried water. Additionally, there is a blue shift (Table 4) in the peak of librational motions by about 8−9 cm^{-1} going from bulk to surface water and by 20−30 cm^{-1} going from bulk to buried water. The structure of the fully protonated PAMAM dendrimer (low pH) is much more opened (Figure 1), and there is a gradual decrease in diffusion and blue shift (Figure 4e) in the libration from the bulk (37 cm^{-1}), to surface (46 cm^{-1}), and to buried (58 cm^{-1}) water. Such blue shift of the water libration is also observed by Pal et al. in their simulation study of water near a micelle of cesium perfluorooctanoate surfactant.[25] The numerical values of translational diffusion coefficients of water in different domains are listed in Table 5. The reductions of D_T from the bulk to surface and buried water are 19% and 89%, respectively, for high pH solution. The reductions are 23% and 83% in the case of intermediate pH, and 21% and 67% for low pH solutions. [The D_T of bulk water under high solution pH (6.88×10^{-5} cm^2/s) is 2.8 times larger than the experimental value (2.5×10^{-5} cm^2/s). This discrepancy is likely a result of the use of a none periodic system in our simulation. We have independently performed a constant temperature (300 K) and pressure (0 GPa) simulation for a system of 612 water molecules in a periodic cell. The translational diffusivity determined from 5 pieces of 20 ps trajectories is found to be (2.70 ± 0.26) $\times 10^{-5}$ cm^2/s, in good agreement with the experimental value. The rotational diffusion determined in this case is (3.14 ± 0.25) $\times 10^{11}$ l/s, slightly higher than the experimental value of 2.2×10^{11} l/s.]

The rotational spectrum shows a somewhat different variation compared to the case of the translational modes. For the unprotonated PAMAM dendrimers (Figure 4b), the rotational mode distributions for the surface and the bulk water are rather similar. This indicates that the water rotations are not much affected by the presence of the PAMAM dendrimer. However, the buried water show a much lower rotational diffusion (smaller $S_R(0)$) and a blue shift of the libration peak (Table 4) by 36 cm^{-1} (from 496 cm^{-1} for the bulk water to 532 cm^{-1} for the buried water). The difference in the rotational dynamics of water in different domains increases as the protonation level increases. For the case when primary amines are protonated (Figure 4d), the blue shift from bulk is 33 cm^{-1} for the surface water and 46 cm^{-1} for the buried water. For the fully protonated PAMAM

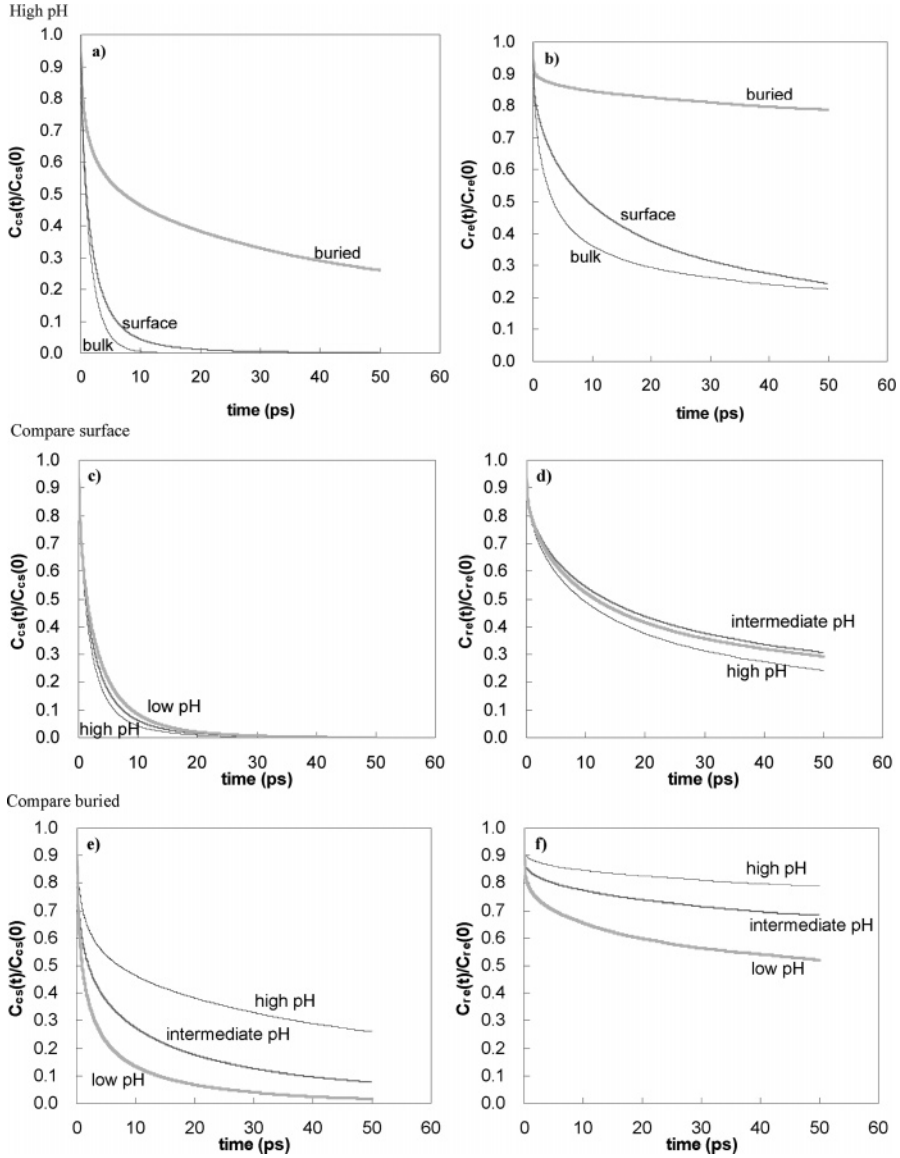

Figure 3. The time correlation function of water from the domain analysis: (a) high pH, eq 1; (b) high pH, eq 2; (c) surface water, eq 1; (d) surface water, eq 2; (e) buried water, eq 1; and (f) buried water, eq 2.

(Figure 4f), the blue shift in rotational libration increases to 35 cm^{-1} for the surface water and 56 cm^{-1} for the buried water. The reduction of rotational diffusion (Table 5) is quite similar to that for the translational diffusion. For high pH, the reduction from bulk water is 22% for surface water and 79% for buried water. The corresponding reductions are 28% and 73% for intermediate pH, and 20% and 55% for low pH solutions.

The effect of protonation of PAMAM dendrimer on the water dynamics can be seen from the comparison shown in Figure 5. For the buried water (Figure 5a), the higher protonation of PAMAM results in an increase in the translational diffusion and a slight red shift (unprotonated 67 cm^{-1}, primary amine protonated 61 cm^{-1}, fully protonated 58 cm^{-1}) of the libration peak. This indicates that as the solution pH is lowered and the PAMAM structure becomes more open, the buried water becomes more mobile. The rotational diffusion (Figure 5b) appears to be independent of the level of PAMAM protonation while there is a significant blue shift in the rotational libration at high protonation (unprotonated 532 cm^{-1}, primary amine protonated 557 cm^{-1}, fully protonated 567 cm^{-1}). Therefore the protonation of amines on PAMAM leads to a more strained water rotation. For the surface water (Figure 5c,d), the primary amine protonation results in a reduction in both translational and rotational diffusion but further tertiary amine protonation does not cause further reduction in the diffusion or the libration peak shift. These results indicate that the protonation of primary amines greatly changes the surface properties of PAMAM, causing the water diffusion to slow and libration to be more strained. However, protonation on tertiary amines located at the buried part of PAMAM dendrimer does not lead to a further change of the surface properties.

Summarizing these results, we find that the dynamical behavior of water is affected by both the PAMAM−water interaction as well as the spatial confinement inside the PAMAM cavities. The water in contact with the PAMAM surface diffuses slowly and is more strained. Inside the PAMAM dendrimer the water diffusion is much slower and the librations are much more strained as well. Interestingly, the rotational dynamics of water appears to be affected more by the spatial confinement than the PAMAM−water interactions. This is evident from the fact that the rotational spectrum of the surface and bulk water are very similar but the rotational spectrum of bulk and buried water are distinctly different. The spatial confinement also leads to a slower rotational diffusion and higher strained libration.

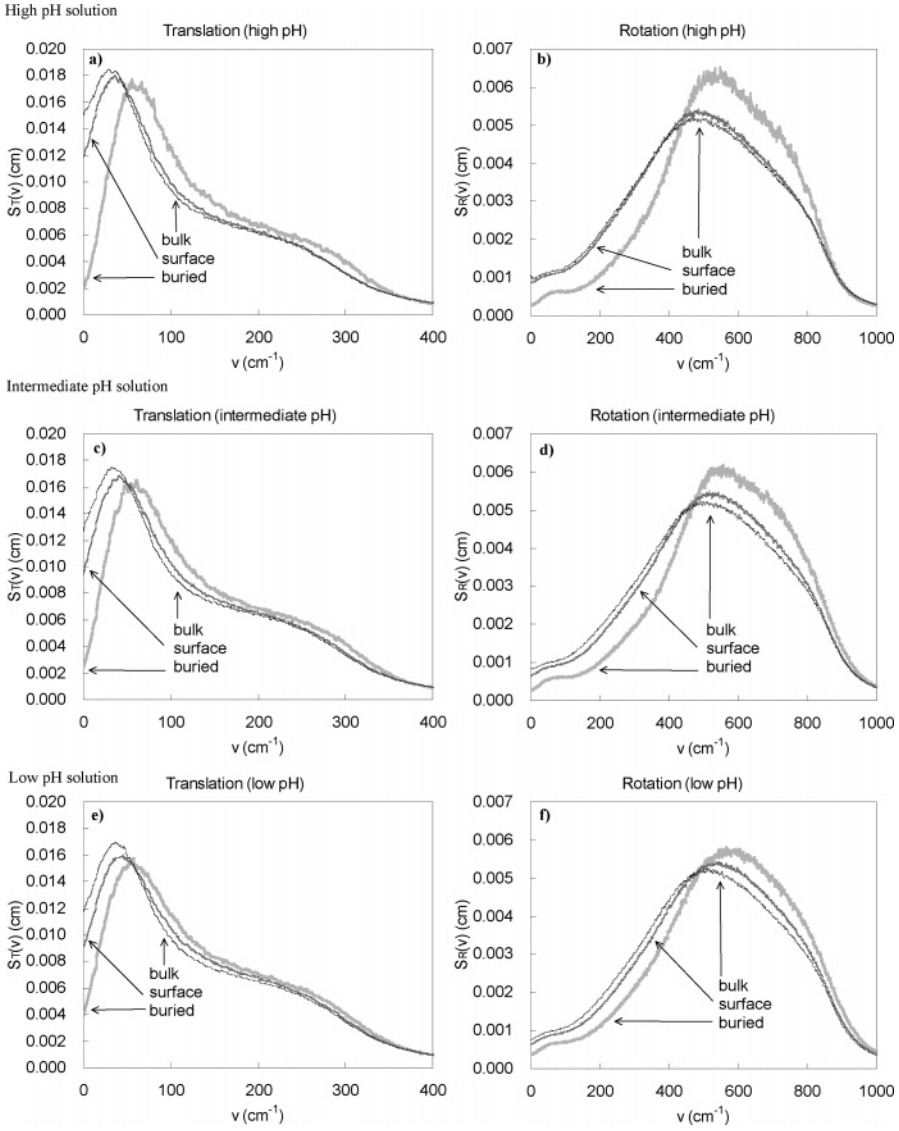

Figure 4. Comparison of the translational and rotational spectra of water in different domains around PAMAM dendrimers: (a) $S_T(v)$, high pH; (b) $S_R(v)$, high pH; (c) $S_T(v)$, intermediate pH; (d) $S_R(v)$, intermediate pH; (e) $S_T(v)$, low pH; and (f) $S_R(v)$, low pH.

TABLE 4: Location of the Peak of Librational Mode Distribution

	domain		
solution pH	buried	surface	bulk
	translation (cm^{-1})		
high	67	37	29
intermediate	61	41	32
low	58	46	37
	rotation (cm^{-1})		
high	532	501	496
intermediate	557	544	511
low	567	546	511

TABLE 5: Translational and Rotational Diffusion Coefficient of Water

	domain		
solution pH	buried	surface	bulk
	translational diffusion ($\times 10^5$ cm^2/s)		
high	0.75 ± 0.03	5.58 ± 0.02	6.88 ± 0.03
intermediate	0.97 ± 0.04	4.33 ± 0.04	5.62 ± 0.02
low	1.71 ± 0.21	4.11 ± 0.04	5.20 ± 0.02
bulk (MD)[a]			2.70 ± 0.26
bulk (exptl)[b]			2.50
	rotational diffusion ($\times 10^{-11}$1/s)		
high	2.17 ± 0.02	8.02 ± 0.09	10.22 ± 0.46
intermediate	2.11 ± 0.06	5.52 ± 0.01	7.69 ± 0.16
low	3.08 ± 0.39	5.45 ± 0.03	6.81 ± 0.04
bulk (MD)[a]			3.14 ± 0.25
bulk (exptl)[b]			2.2

[a] Results from a simulation using 612 F3C water molecules in a periodic cell. [b] Experimental data from ref 13.

The effect of protonation of amines on PAMAM leads to further slowing down in both rotational and translational diffusion, and a higher strained libration of water nearby the proton. Because the primary amines are quite uniformly distributed[8] within PAMAM, their protonation leads to the change of dynamics of water at the surface and inside the dendrimer. In contrast, since tertiary amines are found mostly in the buried regime of PAMAM, their protonation has a strong effect on the buried water but not on the surface ones.

3.4. Thermodynamic Properties of Water. Table 6 summarizes the thermodynamic properties of the water molecules in different domains. The energies listed (also shown in Figure 6) are the strain energies determined from distributing the total system energy to each atom and summing the contributions for water molecules under consideration. Due to the presence of Cl^- in the bulk water, the water energies are slightly lower for

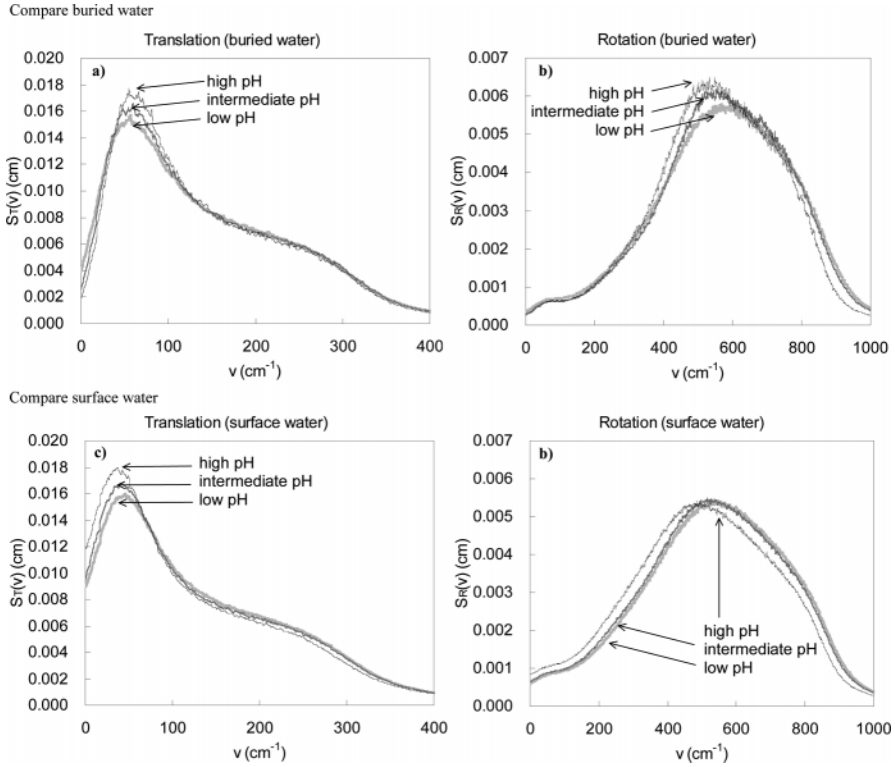

Figure 5. Comparison of the translational and rotational spectrum of water around PAMAM at different solution pH values: (a) S_T(v), buried water; (b) S_R(v), buried water; (c) S_T(v), surface water; and (d) S_R(v), surface water.

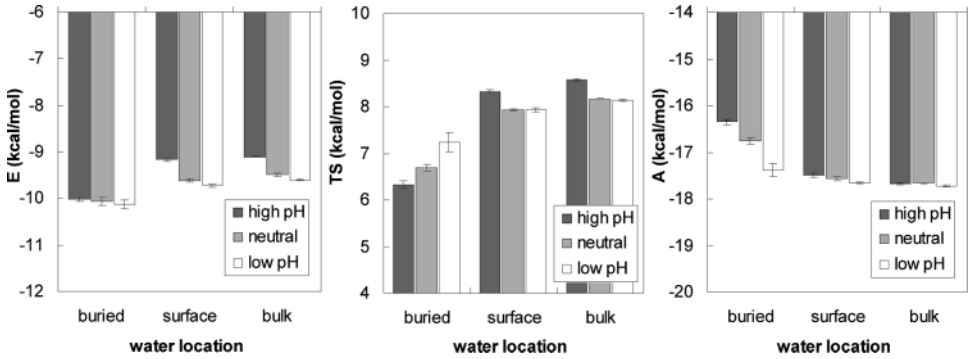

Figure 6. Comparison of energy (*E*), entropy (*S*), and Helmholtz free energy (*A*) of water in different domains around PAMAM at different solution pH values.

TABLE 6: Thermodynamic Properties of Water in Different Environments

	domain		
solution pH	buried	surface	bulk
	energy *E* (kcal/mol)		
high	-10.02 ± 0.04	-9.17 ± 0.03	-9.10 ± 0.01
intermediate	-10.07 ± 0.09	-9.62 ± 0.03	-9.50 ± 0.03
low	-10.14 ± 0.09	-9.72 ± 0.03	-9.60 ± 0.01
	entropy TS (kcal/mol)		
high	6.33 ± 0.07	8.33 ± 0.03	8.57 ± 0.03
intermediate	6.69 ± 0.07	7.94 ± 0.02	8.17 ± 0.02
low	7.24 ± 0.22	7.93 ± 0.05	8.13 ± 0.02
	free energy $A = E$ - TS (kcal/mol)		
high	-16.35 ± 0.05	-17.50 ± 0.04	-17.68 ± 0.03
intermediate	-16.76 ± 0.07	-17.56 ± 0.04	-17.67 ± 0.02
low	-17.38 ± 0.14	-17.66 ± 0.02	-17.73 ± 0.02

the protonated PAMAM cases (the difference is 0.4 kcal/mol between high and intermediate pH solutions and 0.5 kcal/mol between high and low pH solutions). The water energies are about 0.1 kcal/mol lower at the PAMAM surface compared to the bulk, and are lowered by 0.92, 0.57, and 0.54 kcal/mol for buried water for high, intermediate, and low pH conditions, respectively. These results are consistent with the view that the water molecules may form strong hydrogen bonds with the amine groups and protons of PAMAM, therefore lowering the energy. Consequently, water molecules are enthalpically favored at the PAMAM surface and inside the dendrimer. It is interesting to note that our finding of the small alteration in water energetics (0.1 kcal/mol) due to the presence of a macromolecule despite a dramatic change in the water dynamics is similar to that reported by Pal et al. in an aqueous micelle system.[25]

The entropy of water molecules in different environments around the PAMAM dendrimer can be determined by using the 2PT method recently developed by Lin et al.[35] The 2PT method is a modification of the quasiharmonic approximation methods[36−39] where the entropy is determined by treating each mode in the vibrational spectrum $S(\upsilon)$ as a harmonic oscillator. The fluidicity problems, including the singularity in entropy at zero frequency due to diffusion and the anharmonicities at low-frequency regime, are resolved by decomposing the liquid $S(\upsilon)$ into a solid $S^s(\upsilon)$ and a gas $S^g(\upsilon)$ component, and treating each component with appropriate statistics. Lin et al. have shown

that very accurate thermodynamic properties for Lennard-Jones fluid can be obtained from $S(\upsilon)$ by using the trajectory of a length of about 20 ps. In the 2PT method, the entropy is determined by

$$S = \int_0^\infty d\upsilon S^s(\upsilon)\, W_S^{HO}(\upsilon) + \int_0^\infty d\upsilon S^g(\upsilon)\, W_S^{g}(\upsilon) \quad (9)$$

where $W_S^{HO}(\upsilon)$ and $W_S^{g}(\upsilon)$ are the weighting functions of entropy for a harmonic oscillator and a hard sphere gas, respectively

$$W_S^{HO}(\upsilon) = \frac{\beta h\upsilon}{\exp(\beta h\upsilon) - 1} - \ln[1 - \exp(-\beta h\upsilon)] \quad (10a)$$

$$W_S^{g}(\upsilon) = \frac{1}{3}\frac{S^{HS}}{k_B} \quad (10b)$$

with $\beta = 1/kT$, h Plank's constant, and S^{HS} the hard sphere entropy determined by the Carnahan−Starling equation of state.[40] The details of how to decompose $S(\upsilon)$ into $S^s(\upsilon)$ and $S^g(\upsilon)$ can be found in ref 35. Also note that the entropic contribution from molecular rotations is assumed to be a constant value of 44.58 J/(mol K) (3.2 kcal/mol in terms of TS at 300 K) as previous studies have shown that the rotational entropy in solution can be well estimated from the value in the ideal gas condition.[41−43] The vibrational entropies are small and are ignored in our calculation. The 2PT method has been used to determine the various phases of dendrimer liquid crystals[44] and stability of various forms of dendrimer aggregate.[45] In the Appendix we provide a simple validation of the 2PT method for the calculation of free energy of liquid water.

Table 6 and Figure 6 present the calculated entropy (weighted by temperature) from the 2PT method using the vibrational spectrum of water (Figure 4). There is a slight (0.19 to 0.25 kcal/mol) decrease of entropy for water going from the bulk to the surface, and depending on the protonation level of PAMAM a further (0.69 to 1.99 kcal/mol) decrease of entropy of water going from the surface to the buried part of the dendrimer. Therefore, though the water molecules are energetically favored around PAMAM, they are entropically unfavored (leading to an increase of free energy) at the surface or interior of the PAMAM dendrimer. The net effect is a higher free energy state for water surrounding PAMAM dendrimers.

The free energies of water in different environments are presented in Figure 6. At high solution pH, the free energy of the water at the PAMAM surface is 0.18 kcal/mol higher than that of bulk water. For water inside the PAMAM it is 1.32 kcal/mol higher as compared to that of the bulk water. At intermediate pH, the free energy increases by 0.11 kcal/mol going from bulk water to PAMAM surface, and by 0.91 kcal/mol to the internal of PAMAM. For low pH solutions, the increase of free energies is less significant and is 0.07 and 0.35 kcal/mol, respectively. Therefore, unlike the dramatic changes in water dynamical behaviors at various protonation levels, the protonation of PAMAM makes the distinction of water free energies in different domains less significant.

It should be noted that the entropy calculated from the 2PT method is valid for the time period used to determine the vibrational spectrum, i.e., 20 ps. We are able to estimate the local entropy values of water because, as shown previously, the residence time of water is about 20 ps or longer. If a much longer trajectory were used, a significant amount of water would have exited the domain of interest. In this case the vibrational spectrum would be the average of water motions in different domains and the water properties would be less distinctive in each domain.

4. Conclusion

The unusual dynamical behavior of water in biological systems is important in obtaining a better understanding of the role of water in many interesting biological processes. PAMAM dendrimers constitute a class of polymers in which the branching and length are well-controlled and which have great potential in gene therapy, drug delivery, and even environmental protection. Consequently to better understand the binding of PAMAM with DNA, proteins, or heavy metals, it is useful to study the dynamics and thermodynamics of water around PAMAM dendrimers.

Our simulation results show that the water around PAMAM dendrimers behaves quite similarly to that in biological systems. Two distinct relaxation behaviors are observed for waters at the PAMAM surface and inside the dendrimer. Water diffusion around the dendrimer is significantly reduced and the librational motions are more constrained compared to those of bulk water. Protonation of the amines on PAMAM (lower pH) enhances these effects, suggesting that binding a ligand to PAMAM at low pH may be much slower than that at high pH.

We find little enthalpic difference between waters in the three different domains around PAMAM; however, we find that the entropy decreases significantly (1.5 kcal/mol for high pH) for buried PAMAM compared to the bulk (for surface water the difference is 0.8 kcal/mol at high pH). Therefore, the water molecules near the dendrimer have a higher free energy compared to bulk waters. Upon binding, this free energy is released as the inside or surface waters are exchanged with ligand molecules.

Appendix: Validation of Free Energy Calculation of Liquid Water from the 2PT Method

Here we demonstrate the feasibleness of 2PT in the calculation of free energy of liquid water. A simple test would be to compare the 2PT calculated free energies to those from other methods such as Monte Carlo. However, various Monte Carlo implementations usually give slightly different results; furthermore, we do not find such values for F3C water in the literature. For these reasons, it may be more sensible to compare the pressure calculated from the formal method in molecular simulations, i.e., one-third of the trace of the stress tensor, and from the partial derivative of Helmholtz free energy A with respect to volume V,

$$\left(\frac{\partial A}{\partial V}\right)_T = -P \quad (A1)$$

with A being calculated from the 2PT model. This should also provide a good consistent check because both quantities can be evaluated from the same simulation.

We have performed NVT MD simulations for 216 water molecules at densities ranging from 0.8 to 1.1 g/cm^3 at two temperatures, 298 and 400 K. To obtain a statistical average, at each state point we did 20 independent simulations. For each simulation, we performed 10 ps equilibration followed by 20 ps sampling (for the 2PT free energy calculation). The total entropy of water was calculated by the sum of a constant rotational entropy (44.49 J/(mol K) at 298 K and 48.17 J/(mol K) at 400 K) and the translational contribution determined from the 2PT method. Together with the energy E, we obtained the total Helmholtz free energy A ($=E - TS$). The variation of A

(averaged over 20 independent samples) with density ρ was then fitted to a second-order polynomial (the correlation coefficients R^2 were both found to be greater than 0.99). The 2PT pressures were then obtained from eq A.1.

The comparison of the calculated 2PT pressures with those from the MD output (one-third of the trace of the stress tensor) at temperatures 298 and 400 K is shown below. It is clear that

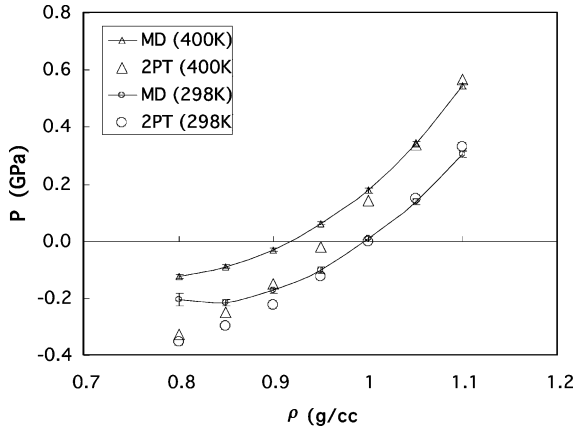

in the stable phase ($P > 0$) the 2PT values are in good agreement with the MD results. Therefore it should be evident that the free energies we obtained here are quite reliable for stable liquid water.

Acknowledgment. This material is based upon work supported by, or in part by, the U.S. Army Research Laboratory, the U.S. Army Research Office under grant no. DAAG55-97-1-0126, and the National Science Foundation under grant no. CTS-0132002. The facilities of the MSC are also supported by grants from NSF, ARO (DURIP), Chevron, General Motors, Seiko Epson, Avery Denison, Asahi Kasei, and Beckman Institute.

References and Notes

(1) Haensler, J.; Szoka, F. C. *Bioconj. Chem.* **1993**, *4*, 372.
(2) Bielinska, A.; KukowskaLatallo, J. F.; Johnson, J.; Tomalia, D. A.; Baker, J. R. *Nucleic Acids Res.* **1996**, *24*, 2176.
(3) Tang, M. X.; Redemann, C. T.; Szoka, F. C. *Bioconj. Chem.* **1996**, *7*, 703.
(4) Balogh, L.; Tomalia, D. A. *J. Am. Chem. Soc.* **1998**, *120*, 7355.
(5) Ottaviani, M. F.; Montalti, F.; Turro, N. J.; Tomalia, D. A. *J. Phys. Chem. B* **1997**, *101*, 158.
(6) Ottaviani, M. F.; Bossmann, S.; Turro, N. J.; Tomalia, D. A. *J. Am. Chem. Soc.* **1994**, *116*, 661.
(7) Esumi, K. Dendrimers for nanoparticle synthesis and dispersion stabilization. In *Colloid Chemistry, Ii*; Topics in Current Chemistry, No. 227; Springer: London, UK, 2003; p 31.
(8) Maiti, P. K.; Cagin, T.; Lin, S. T.; Goddard, W. A., III *Macromolecules* **2005**, *38*, 979.
(9) Maiti, P. K.; Cagin, T.; Wang, G.; Goddard, W. A., III *Macromolecules* **2004**, *37*, 6236.
(10) Maiti, P. K.; Cagin, T.; Li, Y. Y.; Goddard, W. A., III Submitted for publication.
(11) Nandi, N.; Bagchi, B. *J. Phys. Chem. A* **1998**, *102*, 8217.
(12) Nandi, N.; Bagchi, B. *J. Phys. Chem. B* **1997**, *101*, 10954.
(13) Pal, S. K.; Peon, J.; Bagchi, B.; Zewail, A. H. *J. Phys. Chem. B* **2002**, *106*, 12376.
(14) Jimenez, R.; Fleming, G. R.; Kumar, P. V.; Maroncelli, M. *Nature* **1994**, *369*, 471.
(15) Funayama, K.; Imae, T.; Seto, H.; Aoi, K.; Tsutsumiuchi, K.; Okada, M.; Nagao, M.; Furusaka, M. *J. Phys. Chem. B* **2003**, *107*, 1353.
(16) Ruffle, S. V.; Michalarias, I.; Li, J. C.; Ford, R. C. *J. Am. Chem. Soc.* **2002**, *124*, 565.
(17) Pal, S. K.; Zhao, L. A.; Zewail, A. H. *Proc. Natl. Acad. Sci. U.S.A.* **2003**, *100*, 8113.
(18) Bhattacharyya, K. *Acc. Chem. Res.* **2003**, *36*, 95.
(19) Luise, A.; Falconi, M.; Desideri, A. *Proteins-Struct. Funct. Genetics* **2000**, *39*, 56.
(20) Marchi, M.; Sterpone, F.; Ceccarelli, M. *J. Am. Chem. Soc.* **2002**, *124*, 6787.
(21) Rocchi, C.; Bizzarri, A. R.; Cannistraro, S. *Phys. Rev. E* **1998**, *57*, 3315.
(22) Dastidar, S. G.; Mukhopadhyay, C. *Phys. Rev. E* **2003**, *68*, 021921.
(23) Balasubramanian, S.; Pal, S.; Bagchi, B. *Phys. Rev. Lett.* **2002**, *89*, 115505.
(24) Tarek, M.; Tobias, D. J. *Biophys. J.* **2000**, *79*, 3244.
(25) Pal, S.; Balasubramanian, S.; Bagchi, B. *Phys. Rev. E* **2003**, *67*, 061502.
(26) Bagchi, B. *Annu. Rep. Prog. Chem. Sect. C* **2003**, *99*, 127.
(27) Cagin, T.; Wang, G. F.; Martin, R.; Breen, N.; Goddard, W. A., III *Nanotechnology* **2000**, *11*, 77.
(28) Levitt, M.; Hirshberg, M.; Sharon, R.; Laidig, K. E.; Daggett, V. *J. Phys. Chem. B* **1997**, *101*, 5051.
(29) Lee, I.; Athey, B. D.; Wetzel, A. W.; Meixner, W.; Baker, J. R. *Macromolecules* **2002**, *35*, 4510.
(30) Mayo, S. L.; Olafson, B. D.; Goddard, W. A., III *J. Phys. Chem.* **1990**, *94*, 8897.
(31) Rappe, A. K., Goddard, W. A., III *J. Phys. Chem.* **1991**, *95*, 3358.
(32) Ding, H. Q.; Karasawa, N.; Goddard, W. A., III *J. Chem. Phys* **1992**, *97*, 4309.
(33) Lim, K.-T.; Brunett, S.; Iotov, M.; McClurg, R. B.; Vaidehi, N.; Dasgupta, S.; Taylor, S.; Goddard, W. A., III *J. Comput. Chem.* **1997**, *18*, 501.
(34) Berens, P. H.; Mackay, D. H. J.; White, G. M.; Wilson, K. R. *J. Chem. Phys.* **1983**, *79*, 2375.
(35) Lin, S. T.; Blanco, M.; Goddard, W. A. I. *J. Chem. Phys.* **2003**, *119*, 11792.
(36) Schlitter, J. *Chem. Phys. Lett.* **1993**, *215*, 617.
(37) Schäfer, H.; Daura, X.; Mark, A. E.; van Gunsteren, W. F. *Proteins-Struct. Funct. Genetics* **2001**, *43*, 45.
(38) Schäfer, A.; Klamt, A.; Sattel, D.; Lohrenz, J. C. W.; Eckert, F. *Phys. Chem. Chem. Phys.* **2000**, *2*, 2187.
(39) Karplus, M.; Kushick, J. N. *Macromolecules* **1981**, *14*, 325.
(40) Carnahan, N. F.; Starling, K. E. *J. Chem. Phys.* **1970**, *53*, 600.
(41) Mammen, M.; Shakhnovich, E. I.; Deutch, J. M.; Whitesides, G. M. *J. Org. Chem.* **1998**, *63*, 3821.
(42) Guggenheim, E. A. *Trans. Faraday Soc.* **1941**, *37*, 97.
(43) Wertz, D. H. *J. Am. Chem. Soc.* **1980**, *102*, 5316.
(44) Li, Y. Y.; Lin, S. T.; Goddard, W. A., III *J. Am. Chem. Soc.* **2004**, *126*, 1872.
(45) Lin, S. T.; Jang, S. S.; Cagin, T.; Goddard, W. A., III *J. Phys. Chem. B* **2004**, *108*, 10041.